Atmospheric
Chemistry
and Physics
Discussions

Open Access

Particulate organic nitrates observed in an oil and natural gas production region during wintertime

L. Lee[1], **P. J. Wooldridge**[1], **J. deGouw**[2], **S. S. Brown**[2], **T. S. Bates**[3], **P. K. Quinn**[4], **and R. C. Cohen**[1,5]

[1]Department of Chemistry, University of California, Berkeley, CA, USA
[2]Chemical Science Division, Earth System Research Laboratory, National Oceanic & Atmospheric Administration, Boulder, CO, USA
[3]Joint Institute for the Study of the Atmosphere and Ocean, University of Washington, Seattle, WA, USA
[4]Pacific Marine Environment Laboratory, National Oceanic & Atmospheric Administration, Seattle, WA, USA
[5]Department of Earth and Planetary Sciences, University of California, Berkeley, CA, USA

Correspondence to: R. C. Cohen (rccohen@berkeley.edu)

Discussion Paper | Discussion Paper | Discussion Paper | Discussion Paper

Title Page

Abstract	Introduction
Conclusions	References
Tables	Figures

|◄ | ►|
◄ | ►
Back | Close

Full Screen / Esc

Printer-friendly Version

Interactive Discussion

L. Lee et al.

Abstract

Organic nitrates in both gas and condensed (aerosol) phases were measured during the Uintah Basin Winter Ozone Study from January to February in 2012. A high degree of correlation between total aerosol volume at diameters less than 500 nm and the particulate organic nitrate concentration indicates that organic nitrates are a consistent, if not dominant, fraction of fine aerosol mass. In contrast, a similar correlation with sub 2.5 μm aerosol volume is weaker. The C : N atomic ratio inferred from field measurements of $PM_{2.5}$ and particulate organic nitrate is 34 : 1. Calculations constrained by the observations indicate that both condensation of gas phase nitrates and heterogeneous reactions of NO_3 / N_2O_5 are responsible for introducing organic nitrate functionality into the aerosol and that the source molecules are alkanes. Extrapolating the results to urban aerosol suggests organic nitrate production from alkanes may be a major secondary organic aerosol source.

1 Introduction

Sub-micron sized aerosol affect the global radiative balance directly as a result of variation in their optical properties and indirectly via their effect on clouds. They modulate atmospheric composition by scavenging gas phase material, including oxidants. The aerosol impact visibility and public health (Hallquist et al., 2009; Went, 1960; Kleinman et al., 1995). Observations have shown that micron sized aerosol typically contain ∼ 50 % organic material by mass (Zhang et al., 2007), and the sources of these organic aerosol have been the subject of considerable debate (Bahreini et al., 2012; Gentner et al., 2012; Shilling et al., 2013; Worton et al., 2013). Field observations have found organic aerosol in urban areas to correlate with anthropogenic emissions, and that they are formed in the atmosphere through chemical reactions of gaseous precursors (Hallquist et al., 2009). However, It has also been shown that urban organic aerosol contains significant amount of carbon that is "modern" (Lewis et al., 2004; Szidat et al.,

2004; Zhang et al., 2013), i.e., from a biological source, such as biogenic emissions or biomass burning. It remains challenging to explain secondary organic aerosol (SOA) produced from modern carbon but controlled by anthropogenic emissions (Weber et al., 2007). Nitrogen oxides (NO_x) are possible candidates for modulating aerosol formation as they are primarily anthropogenic so that an aerosol formation pathway mediated by NO_x may explain this seemingly counter intuitive phenomenon in terms of radiocarbon age. One potential tracer for this process is organic nitrates in aerosol.

Recently, methods to identify organic nitrate in ambient aerosol have become available. Observations in chamber studies of the NO^+/NO_2^+ peaks in aerosol mass spectrometer measurements (Rollins et al., 2009, 2010a; Farmer et al., 2010), by Fourier Transform Infrared Spectroscopy (FTIR) of ambient aerosol (Day et al., 2010; Mylonas et al., 1991; Garnes and Allen, 2002) and by Thermal Dissociation-Laser Induced Fluorescence (TD-LIF) of ambient aerosol (Rollins et al., 2010b, 2012, 2013) indicate that organic nitrates in ambient aerosol are observable, and that there are mechanisms to produce them in significant yields from common organic precursors. For example, in Bakersfield, California during summer, Rollins et al. (2012) found that aerosol-bound organic nitrate production contributed to as much as 30 % of the aerosol growth rate at night with nitrooxy group representing 8.4 % of the growth mass.

Recent studies of organic matter in ambient aerosol have focused on anthropogenic emissions of gasoline, diesel (Gordon et al., 2013; Jathar et al., 2013; Gentner et al., 2012; Bahreini et al., 2012), motor oil (Worton et al., 2014) and biogenic VOCs (Brown et al., 2009; Paulot et al., 2009; Froyd et al., 2010) as precursors. For long chain aliphatics, laboratory experiments and simulations have demonstrated substantial contribution of organic nitrates in the resulting particulate matter (Jordan et al., 2008; Lim and Ziemann, 2009; Matsunaga and Ziemann, 2010), but there exist few field observations capable of assessing whether these mechanisms are representative of the ambient processes. Here we describe observations of organic nitrate aerosol observed in the Uintah Basin, Utah during winter 2012. The measurement site is heavily influenced by oil and gas drilling operations and has negligible input of biogenic emissions, providing

an excellent opportunity to explore the role of organic nitrates formed from aliphatic compounds in the production of ambient aerosol.

2   Methods

Observations of NO_2, total organic nitrates and particulate organic nitrates (pΣAN) were made as part of the Uintah Basin Winter Ozone Study (UBWOS) in January and February of 2012. The instruments were installed on a 19 m tower located on an operational oil and gas well pad containing a wellhead for water injection with a nearby unpaved access road. The measurement site (40.14370° N, 109.46718° W) is approximately 30 miles south of Vernal, the nearest town in Utah. The aerosol measurements that are the focus of this manuscript were made from inlets 9 m above the ground.

NO_2, total organic nitrates and pΣAN were measured by TD-LIF with coupling to an inlet denuder as described in Rollins et al. (2010). TD-LIF is described in detail elsewhere (Day et al., 2002; Thornton et al., 2000). Briefly, in these experiments a CW 408 nm solid state diode laser (Power Technology Inc., LDCU12/7639) was used to excite NO_2 molecule. The laser light was directed sequentially into 3 multi-pass white cells and total fluorescence due to NO_2 at wavelengths longer than 700 nm was detected using a red-sensitive photomultiplier tube (Hamamatsu H7421-50) behind dielectric filters that set the transmission window. The cell pressure was maintained at 3 Torr.

Simultaneous detection of organic nitrate species was effected by quantitative conversion of alkyl nitrate ($-ONO_2$) and peroxy nitrate ($-OONO_2$) moiety to NO_2 molecule through thermal decomposition at 17 ms residence time under 380 °C in a 0.25 inch OD quartz tube. The sampled air contained both gas phase and aerosol phase organic nitrates which, upon passing through the thermal dissociation (TD) oven, were converted into an excess NO_2 signal compared to the ambient NO_2 concentration monitored simultaneously in an unheated channel. To distinguish the particulate phase component, an activated charcoal multi-channel denuder of 10 cm in length (MAST Carbon Inc.) was placed ahead of another 380 °C TD oven to remove the gas phase organics

(Rollins et al., 2010b) as well as NO_2 so that only aerosol phase component remained. The particle transmission efficiency of the denuder was calculated to be 60 % for 20 nm diameter particles and over 90 % for particles larger than 70 nm diameter, ensuring detection of the vast majority of aerosol mass. To reduce intake of dust, a 2.5 µm cyclone

5 was placed on the main inlet with a bypass pump maintaining the necessary total flow rate of 5 L per minute. In addition to these TD-LIF measurements, N_2O_5 (Wagner et al., 2011), peroxy acetyl nitrate (PAN) (Williams et al., 2000) and $ClNO_2$ (Roberts et al., 2009) were independently measured. Total alkyl nitrate (ΣAN) is defined as the measured TD-LIF signal at 380 °C, corrected for ozone effects (Lee et al., 2014) and with

10 NO_2, N_2O_5, PAN and $ClNO_2$ subtracted. The particle organic nitrate observations require no correction as gas phase molecules are scrubbed by the denuder. We expect alkyl nitrates to be the dominant component of the particulate organic nitrate signal observed, because the peroxy nitrate concentration as well as the concentration of their precursors are much lower than the corresponding alkyl nitrates.

15 The TD-LIF instrument was calibrated hourly using locally generated zero air mixed with an NO_2 standard to give 5 different concentration levels, spanning a range from 0 to 20 ppb. The instrument zero was monitored twice per hour. Concentration data were reported to the NOAA archive (http://esrl.noaa.gov/csd/groups/csd7/measurements/2012ubwos/) at a time resolution of 1 min, averaged from 1 Hz raw data. The detec-

20 tion limit for the instrument at 1 min averaging time was 24 ppt for NO_2 and particulate nitrate and 34 ppt for total organic nitrate, defined as the $1 - \sigma$ value of the noise. The charcoal denuder was occasionally checked for saturation by introducing the calibration NO_2 gas mixture before, rather than after, the denuder section in a calibration routine, and no NO_2 break-through was observed.

25 Co-located aerosol instrumentations include measurements of the particle size distribution from 10 to 500 nm diameter range using a scanning mobility particle sizer (SMPS, TSI Inc.), from 0.7 to 10 µm diameter range using an aerodynamic particle sizer (APS, TSI Inc.) and an aerosol mass spectrometer (AMS, Aerodyne Inc.). Sub 2.5 µm aerosol filter samples were collected twice daily, one covering daytime

and one covering nighttime. Properties derived from these filter samples include total aerosol mass, total organic carbon (OC), total elemental carbon (EC) and cation concentrations (ion chromatography). Particle-into-liquid sampler (PILS) was co-located with the filter sampler. Meteorological conditions were recorded at the top of the 19 m tower including wind direction, wind speed, temperature, pressure and relative humidity. Gas phase measurements used in this analysis include gas chromatography with mass selective detector (GC-MS) and proton transfer mass spectrometry (PTR-MS) for VOC speciation, cavity ring-down spectroscopy (CRDS) for N_2O_5 and NO_3, chemical ionization mass spectrometry (CIMS) for $ClNO_2$, and gas chromatography with electron capture detection (GC-ECD) for PAN. (For a comprehensive list, see: http://esrl.noaa.gov/csd/groups/csd7/measurements/2012ubwos/instruments.html.)

3 Observations

The concentration of total organic nitrates (including the contribution from $ClNO_2$ and N_2O_5) and particulate nitrates (pΣANs) are shown in Fig. 1. After correcting for PAN, $ClNO_2$ and N_2O_5, ΣANs account for an afternoon peak of 40 % NO_y and exhibit a strong diurnal pattern, reaching a median value of 2.2 ppb at local noon as shown in Fig. 2. At night high concentrations of N_2O_5 and $ClNO_2$ (∼ 0.6 ppb combined) were present and ΣANs decreased to approximately 300 ppt. PAN was about 250 ppt at night increasing to 400 ppt in the late afternoon. A median value of 45 ppt pΣANs was observed with peak value around 150 ppt (Fig. 1). The level of pΣAN varied more slowly than ΣANs, except at times of pristine air intrusion during which its concentration decreased promptly. From a multi-day perspective, pΣANs were observed to accumulate during stagnant periods as did long-lived trace gases including VOCs, NO_2 and ΣANs.

pΣAN was correlated with other aerosol measurements, the strongest of which ($R^2 = 0.72$) was with aerosol volume at diameters below 500 nm (Fig. 3). In contrast, the correlation with total aerosol volume up to 2.5 μm particle diameter is weaker ($R^2 = 0.23$). We believe this is due to the presence of mineral dust in the larger size fraction.

The source of this dust is likely exposed dry soil on the numerous unpaved roads in the surrounding area. Correlations between pΣAN and gas phase species such as propane (R^2 = 0.15) and NO_2 (R^2 = 0.1) are weak.

4 Discussion

4.1 Aerosol composition inferred from observations

The inorganic components observed in aerosol at UBWOS consist of mineral dust, salts and elemental carbon. Since pΣAN data represent condensed phase organic nitrooxy groups, the strong correlation of pΣANs concentration with $PM_{0.5}$ volume is suggestive of the existence of both a significant organic component and a persistent nitrooxy functionality in this size range. Complementary evidence for this observation is obtained by correlating the concentration of aerosol Ca^{2+}, typically found in minerals, with the total aerosol volume at diameters between 500 nm and 2.5 µm. The resulting high correlation (R^2 = 0.78) is in contrast to the one obtained for Ca^{2+} with the $PM_{0.5}$ volume (R^2 = 0.03), again lending support to the assumption that the organic particles dominate the particle size range under 500 nm while inorganic components dominate the size range from 500 nm to 2.5 µm.

To obtain a quantitative estimate of organic/inorganic mass in $PM_{2.5}$, linear decomposition of aerosol specific volume was used (Appendix A). The specific volume was calculated as the ratio of $PM_{2.5}$ aerosol volume measured by SMPS and APS divided by $PM_{2.5}$ aerosol mass from impactor filter samples. The use of filter data limits the number of independent estimations to 2 values daily, one during the day and one during the night. This method assumes that inorganic and organic components have distinctive values in density, and they form external mixture in the aerosol phase. The resulting equation relating the observed $PM_{2.5}$ specific volume ($\widetilde{v}$) to aerosol organic

nitrate group mass fraction (f_{ONO_2}) is shown in Eq. (1).

$$\widetilde{v} = \widetilde{v}_{dust} + \left(\widetilde{v}_{org} - \widetilde{v}_{dust}\right) \times (1 + \gamma) \times f_{ONO_2} \qquad (1)$$

$\widetilde{v}_{org}$ and $\widetilde{v}_{dust}$ represent the specific volume of aerosol organic and inorganic compo-
nents, respectively, while γ is the mass ratio of the non-nitrate-containing organics to
the organic nitrate group. Note here that the pΣAN measurement is insensitive to in-
organic nitrate ions and allowed us to use it as an unambiguous tracer for organic
components in the aerosol phase. Equation (1) predicts a linear relationship between
the aerosol specific volume and organic nitrate mass fraction given that organic nitrates
represent a constant fraction in the organic mass, a condition satisfied as demonstrated
in Fig. 4.

The y intercept of a plot of aerosol specific volume vs. organic nitrate mass fraction
gives the specific volume of the inorganic component directly. We obtained a value
of $0.168\,\text{cm}^3\,\text{g}^{-1}$ corresponding to a nominal density of the inorganic component of
$5.95\,\text{g cm}^{-3}$, a value similar to iron(III) oxide ($d = 5.24\,\text{g cm}^{-3}$). Organic molecules with
moderate oxygenation have a density ($\widetilde{v}_{org}^{-1}$) of approximately $0.85\,\text{g cm}^{-3}$ (for exam-
ple: 1-butyl nitrate ($d = 0.882$), *tert*-butyl nitrate ($d = 0.867$), nonanol ($d = 0.827$) and
butanol ($d = 0.81$)). Using this estimate, we obtain a γ value of 11. This constrains
the organic mass associated with organic nitrate group in aerosol to approximately
680 a.m.u. This associated mass estimated from the light component of the ambient
aerosol typically accounts for 53 % of the observed aerosol volume and 14 % of the
aerosol mass.

It is possible to account for the contribution of soluble inorganic salts that are mea-
sured by PILS by subtracting out an inorganic salt component defined by the sum of
NH_4^+, NO_3^- and SO_4^{2-} groups and their average density of $1.76\,\text{g cm}^{-3}$. The sum of
PILS ions can at times account for up to 50 % of $PM_{2.5}$ mass. The adjusted aerosol
volume and mass after the subtraction of salt component is then analyzed using the
same technique as above to extract a heavy and a light component. The R^2 value of

Title Page

Abstract | Introduction

Conclusions | References

Tables | Figures

|◄ | ►|

◄ | ►

Back | Close

Full Screen / Esc

Printer-friendly Version

Interactive Discussion

0.6 for the correlation of specific volume to organic nitrate mass fraction is identical to the correlation presented above. A γ value of 9.6 is derived from this analysis.

We can now constrain the molecular formula of particulate organic components using this corrected γ value derived above. Together with aerosol mass spectrometer observations during high aerosol loading periods of an $O:C$ value of 0.2 (S. Murphy, private communication, 2013) and a generic chemical formula containing carbon, oxygen, hydrogen and organic nitrate ($-ONO_2$) of the form $(CH_2)_nO_m$ ($HONO_2$) for a fully saturated molecule, we derive an elemental ratio of $C:H:O:N = 34:69:10:1$. Note that any linear combination of organic molecule mixtures giving the same average $C:H:O:N$ ratio can satisfy this constraint, and may consist of both nitrates and non-nitrates.

The range of $C:H:O:N$ ratios consistent with the observations can be estimated from the confidence interval associated with the slope and intercept of the linear regression in Fig. 4. At 95 % confidence interval, we estimate the uncertainty of the γ value to be ± 17 %, given an organic matter density of $0.85\,\mathrm{g\,cm^{-3}}$. We point out that the large uncertainty in the y-intercept does not contribute significantly to the uncertainty of the result because the difference in specific volume is dominated by the organic component. Propagating this range gives $C:H:O:N$ ratio between $28:57:9:1$ and $40:81:11:1$. Note that although the estimated carbon number appears to be high relative to the implied carbon number for organic aerosol generated from the Deepwater Horizon plume (de Gouw et al., 2011), our estimate is relative to the organic nitrate functional group in the aerosol phase. The implication is that not all organics responsible for organic aerosol formation during UBWOS contained organic nitrate groups.

4.2 Daytime production

In the following section we attempt to close the daytime pΣAN budget using gas phase oxidation of aliphatic molecules followed by partitioning of oxidation products into aerosol phase.

pΣAN is thought to be exclusively secondary. Consider daytime processes in the alkane-rich environment observed during UBWOS: the oxidation of an organic molecule R starts with a reaction with OH radical. For a simplified schematic (Reactions 1 and 2) of a single oxidation step in the presence of NO, two generic products are formed with relative yields governed by the organic nitrate yield α.

$$\alpha \qquad R + OH \rightarrow R(ONO_2) \tag{R 1}$$
$$(1 - \alpha) \quad R + OH \rightarrow RO. \tag{R 2}$$

The simple alkyl nitrate $R(ONO_2)$ and products formed from the subsequent reactions of alkoxy radical RO. are assumed to partition into the aerosol phase as a function of their respective vapor pressure. If the partitioning follows ideal solution behavior within the existing aerosol organics, the fraction of the organic products expected to end up in the condensed phase is represented as K_p in Eq. (2), where P^* represents the saturation vapor pressure of the organic molecule, N_{org} the amount of organic molecules in the condensed phase in $mol\,m^{-3}$ and k_B as Boltzmann's constant.

$$K_p = \frac{1}{1 + \frac{P^*}{N_{org}k_BT}} \tag{2}$$

The largest alkane reported during UBWOS 2012 was undecane ($C_{11}H_{24}$). We extrapolate the OH reactivity of larger alkanes using a power law, by fitting a linear relationship ($R^2 = 0.99$) to the observed $C_9 \sim C_{11}$ alkane reactivity in the log space. This approximation combines the decay in gas phase concentration due to reduction in vapor pressure and the increase in alkane OH reactivity with alkane size to generate a complete set of alkane consumption rates due to OH reactions. We then estimate the properties of the OH oxidation products from alkanes using a simplified scheme of 3 species for each carbon number group: an alkyl nitrate, a hydroxy nitrate and a hydroxy carbonyl, with branching ratios of α, $(1 - \alpha)\alpha$ and $(1 - \alpha)^2$, respectively as detailed in Appendix B. The absolute contribution of each type of oxidation product to aerosol formation is therefore

the individual formation rate weighted by K_p. The total aerosol yield attributable to this mechanism is obtained by summing the yield over all carbon number groups above C_6. We used α values estimated with the method by Carter and Atkinson (Carter and Atkinson, 1989) updated by Arey et al. (2001) at the appropriate temperature and pressure.

5 The saturation vapor pressure P^* of the reaction products follows the parameterization of SIMPOL.1 (Pankow and Asher, 2008).

Using this procedure, we calculate the particulate nitrate formation rate for the daytime period of 30 January, during which time the aerosol loading peaked at $2\,\mu g\,m^{-3}$. Using an approximate daytime OH concentration of $10^6\,1\,cm^{-3}$ (Edwards et al., 2013), 10 the total production rate of aerosol phase organic nitrate groups is $3.4\,ppt\,h^{-1}$. The condensable molecules responsible for carrying the nitrooxy groups into the aerosol phase have carbon chain lengths in the range of C_{10} to C_{17}, as shown in Fig. 5. The representative $C:H:O:N$ ratio of aerosol organics predicted by this alkane-only estimation is $18:37:5:1$, or a non-nitrate to nitrate mass ratio of $4.5:1$. This is about half 15 of the value inferred directly from observations ($\gamma = 9.6$). One possible explanation for the difference is that approximately half of the non-nitrate carbonaceous component originates from oxidation of aromatic compounds ($\sim 10\,\%$ of alkanes OH reactivity) or primary sources. Uncertainties in the saturation vapor pressure, and deviation from ideal solution behavior may also contribute.

20 The result obtained above only utilizes the alkane composition data. Independently, the total production rate of pΣAN can be calculated using time series of the measured pΣAN concentration, by solving the mass balance equation (Eq. 3).

$$p\,(p\Sigma AN) = \frac{d(p\Sigma AN)}{dt} + k_{mix} \times p\Sigma AN \qquad (3)$$

Briefly, the total production rate of pΣAN (p(pΣAN)) is the rate of change of pΣAN con-25 centration plus the loss rate. The loss is represented as a first order process with a loss rate constant k_{mix} ($1\,s^{-1}$) which can be estimated using the known production rate and concentration of n-propyl nitrate as a tracer (Lee et al., 2014). Turbulent mixing out of the basin was the dominant driver of k_{mix}. The inferred production rate during the same

daytime period as the above analysis is $3.6\,\mathrm{ppt\,h^{-1}}$, nearly identical to the estimate using alkane composition. It is noted that by assuming the same loss characteristics as n-propyl nitrate, the effect of dry deposition is likely underestimated. Alternatively, the pΣAN formation rate calculated using loss characteristics of HNO_3 yields a daytime production rate that is 21 % higher ($4.4\,\mathrm{ppt\,h^{-1}}$). This is likely an upper limit.

4.3 NO_3/N_2O_5 chemistry

In addition to daytime source of pΣANs, nighttime chemical production may also be important. The dominant reactions are typically those initiated by NO_3 and N_2O_5 radicals, either through gas phase oxidation followed by condensation, or through heterogeneous reactions on the surface of existing organic aerosol. Due to cold temperatures that make gas phase reactions of NO_3 less important by shifting the equilibrium towards N_2O_5 as well as the scarcity of unsaturated hydrocarbons observed, the condensation pathway is likely unimportant. Multiple lab studies on both environmental and synthesized aerosol particles (Gross et al., 2009; Zhao et al., 2011a, b; Xiao and Bertram, 2011; Bertram et al., 2009) have demonstrated that the reactive uptake of NO_3 or N_2O_5 can be significant, and for certain class of organics molecules (e.g. alkenes and alcohols) can give high yield of organic nitrates as condensed phase products. As opposed to daytime analysis, it is difficult to directly estimate the net nocturnal pΣAN production with Eq. (3) due to lack of concentration variation and difficulty in estimating the loss term. However, we found that inclusion of heterogeneous production is necessary to explain the nighttime concentration of pΣAN and we characterize the heterogeneous reactions in the following modeling section.

4.4 Modelling the aerosol time series

A box model incorporating the above daytime and nighttime mechanisms was used to simulate the organic nitrate content of the aerosol.

Particulate organic nitrates observed in an oil and natural gas production region

L. Lee et al.

Title Page

Abstract	Introduction
Conclusions	References
Tables	Figures

|◄ | ►|

◄ | ►

Back | Close

Full Screen / Esc

Printer-friendly Version

Interactive Discussion

The observed ΣAN is assumed to represent the total concentration of organic nitrates produced due to photochemistry as described in Lee et al. (2014), with an effective saturation vapor pressure as a tuning parameter to determine the effective partitioning based on Eq. (2). The bi-directional exchange is calculated according to gas kinetic theory and detailed balance derived from the saturation vapor pressure accounting for the Kelvin effect.

For the nighttime chemistry, we introduce a new parameter, the retaining coefficient (ζ), defined as the probability of reactive uptake yielding condensed phase organic nitrates given a gas molecule-surface collision. This differs from the reactive uptake coefficient by excluding non-nitrate forming channels. The pΣAN production is calculated from gas molecule-surface collision rate corrected for diffusion transport and then multiplied by ζ. The organic nitrates formed through this pathway are assumed to remain in the condensed phase.

Loss of pΣANs is assumed to follow the loss of aerosols. The most important process is turbulent mixing with a lifetime of ~ 8 h during daytime periods. The full time series of first order loss rate is calculated using tracer methods (Lee et al., 2014) and applied to the simulation. We used HNO_3 to estimate the loss rate which gives a more realistic loss profile during the evening when the boundary layer is stable.

The resulting time series of predicted concentrations are shown in Fig. 6, where the top panel describes the 2 consecutive accumulation periods and the lower panel extends the simulation to all observations. We find an effective saturation vapor pressure of 26 ppb for the ensemble of total organic nitrate species and NO_3 reactive uptake coefficient ζ_{NO_3} of 0.1 for the full length of simulation. The model is highly correlated with the observations (slope of 0.98 and R^2 value of 0.72) over the 2-week period shown in the top panel of Fig. 6. A reduced correlation with a slope of 0.72 and an R^2 of 0.66 is observed for the full data (bottom panel of Fig. 6). This fitted effective saturation vapor pressure is consistent with one calculated from the VOC speciation (28 ppb ΣANs). The major discrepancies in the extended simulation arise when organic aerosol mass becomes more abundant in the super 0.5 µm size range (up to 36 % of total pΣANs),

particularly during the period from 12 to 21 February. It is possible that organics were present as external coatings on the inorganic minerals of large size particles, leading to an enhanced surface to volume ratio relative to a pure particle of the same organic mass. The result is underestimation in predicted organic nitrate content due to discrepancies in the aerosol mixing state. Also, the possibilities of secondary chemistry in the presence of inorganic salts cannot be ruled out.

The ζ_{NO_3} value of 0.1 should be interpreted as a projection of the overall reactivity onto NO_3 reactions, since NO_3 and N_2O_5 interconvert rapidly and both species may contribute to heterogeneous reactions. Given an observed median NO_3/N_2O_5 ratio of 0.007, the heterogeneous chemistry may be equally satisfied with an N_2O_5-based $\zeta_{N_2O_5}$ of 8×10^{-4}, or any linear combination of the two channels. However, we point out that due to the enhancement of N_2O_5 lifetime as a result of the cold temperature and high NO_x concentrations encountered, the heterogeneous reaction cannot be dominated by NO_3 as this requires a value of ζ_{NO_3} larger than even aerosols made of pure unsaturated organic molecules such as solidified oleic acid ($\gamma_{NO_3} = 0.076$) and conjugated linoleic acid ($\gamma_{NO_3} = 0.08$) as observed in laboratory studies (Gross et al., 2009). Therefore, N_2O_5-dominated heterogeneous reactions with hydroxy groups in the aerosol phase is a more likely source of nighttime pΣAN production, and is within range of reported reactive uptake coefficient measured on surface of glycerol particles ($\gamma_{N_2O_5} = 8.14 \times 10^{-4}$) and wintertime aerosol in Colorado ($\gamma_{N_2O_5} \sim 0.01$) (Wagner et al., 2013). Finally, it is noted that the nocturnal production of pΣANs (6 ppt h^{-1}) does not constitute a significant local sink of NO_3 (production rate of 150 ppt h^{-1}).

5 Implications

Our particulate organic nitrate measurements during wintertime in the Uintah Basin, Utah represent a unique opportunity to characterize the chemistry of alkane-derived SOA under ambient (albeit cold) conditions. This is relevant to environments when anthropogenic activities heavily influence the VOC composition. According to the study

of Gentner et al. (2012), both gasoline and diesel fuel sampled at various locations in California were primarily alkanes, with an overall longer chain length in the diesel fuel. Tailpipe emissions of unburnt diesel fuel as well as motor oil (Worton et al., 2014) may represent the predominant source for large alkanes observed in cities (Boynard et al., 2014). For example, VOC enhancement ratios observed in Los Angeles showed a non-decreasing trend from n-nonane to undecane, the largest alkane reported (Borbon et al., 2013). Similar mixing ratios have also been observed in Sacramento, California (Steiner et al., 2008). This is different from the decreasing trend observed in Utah, where the VOC sources are evaporative, but rather consistent with the composition from direct emissions of liquid diesel for which the distribution of C_{10} to C_{20} alkanes are relatively flat.

We calculated the potential organic nitrate aerosol formation from alkanes using the liquid fuel composition tabulated in the supporting information of Gentner et al. (2012) and the partitioning method detailed in Sect. 4.2 for OH initiated oxidation. OH reaction rates for alkanes larger than dodecane are parameterized (Kwok and Atkinson, 1995). For an organic aerosol loading of $2\,\mu g\,m^{-3}$, the organic nitrate aerosol yield is 14 wt.% for diesel fuel and 0.004 wt.% for gasoline, both calculated at 298 K. Since it was estimated by Gentner that both gasoline and diesel vehicles emit similar amount of VOC by weight in the Bakersfield region (Kern county), of the ratio 44 % (gasoline) to 56 % (diesel), the diesel emission dominates the source strength of particulate organic nitrates. We further estimate the potential pΣAN concentrations according to the mass yield calculated above and tailpipe VOC emission of $7\,\mu g\,m^{-3}$ from diesel vehicles, a number we derived based on the SOA production estimation in Gentner et al. The result is 46 ppt pΣAN due to diesel traffic emissions in the Bakersfield region, a value accounting for 77 % of the observed daytime ambient concentration by Rollins et al. (2013), who reported local pΣAN concentration of ~ 60 ppt during daytime periods of the CalNex-2012 campaign. Contributions from local biogenic precursors as well as fugitive losses from oil and gas productions may account for the remaining particulate

nitrates. However, we point out that photochemical aging is required to achieve the yield from our estimation and the above value should be interpreted as an upper limit.

The above example of particulate organic nitrate production around Bakersfield region illustrates the possibility of distinct pathways responsible between daytime and nighttime periods. The saturated, but much heavier alkanes will contribute during the day from OH oxidation and partition more efficiently into the aerosol phase, while the more reactive but generally lighter biogenic emissions may dominate nighttime production due to NO_3 and N_2O_5 chemistry. This is of particular interest in regions with representative VOCs consisting of a mixture of anthropogenic and biogenic contributions.

6 Conclusion

We present $PM_{2.5}$ particulate organic nitrate concentration measurements obtained in wintertime Utah using TD-LIF technique. Of the median $1\,\mu g\,m^{-3}$ organic aerosol estimated, we found organic nitrate to be a consistent portion of the organic mass occupying predominately in the sub $0.5\,\mu m$ particle size ranges of an average $C:H:O:N$ ratio of $34:69:10:1$, likely as a mixture of C_{10} to C_{17} organic nitrates and oxygenates. With the help of a box model, we demonstrate that the particulate organic nitrate concentration observed can be reproduced by gas phase condensation and heterogeneous chemistry of N_2O_5. Both channels contribute almost equally, consistent with the lack of day/night change observed in condensed phase organic nitrate content. By applying our analysis to the California central valley region, we demonstrate that diesel tailpipe emissions can potentially contribute to a significant portion of ambient particulate organic nitrates observed.

Appendix A: Derivation for aerosol specific volume–nitrate concentration relationship

The third panel in Fig. 1 shows the relative importance of total aerosol volume contributions from particles above or under 500 nm size. While we have demonstrated the relative domination of organic/inorganic component has a rough boundary at 500 nm, simply treating this as a cut-off point will likely lead to non-negligible underestimation of organic component that exists in the over 500 nm size range which contained about half of total $PM_{2.5}$ aerosol volume. We therefore propose a method that utilizes our $PM_{2.5}$ pΣAN data as tracers and without assumptions made on the organic content of the various aerosol size ranges. This method is based on the observation that mineral dust or inorganic salts generally have higher density than organic molecules. Instead of focusing on the metric of density which is not an additive parameter, specific volume (or inverse density in $cm^3 g^{-1}$) is used to factor out the inorganic component by linear combination. Under the particular environment of wintertime Uintah Basin, we assume no significant aqueous phase present. As mineral dust and salt are not typically soluble in organic phase, the total volume of the aerosol can be treated as a linear combination of volumes from individual immiscible components, such as the equations presented below:

$$\widetilde{v} = \sum_i \widetilde{v}_i \times f_i \tag{A1}$$

$$\sum_i f_i = 1 \tag{A2}$$

In Eq. (A1), $\widetilde{v}$ is the overall specific volume of the $PM_{2.5}$ aerosol phase, while $\widetilde{v}_i$ and f_i are specific volume and mass fraction of component i in the aerosol phase, respectively. Mass fractions from all aerosol components should add up to 1 (Eq. A2). We now name 3 components in the aerosol phase to be considered explicitly. First component f_{dust} represent collectively the inorganic component, including mineral dust and salt.

The second and third components both represent the organic phase, but was broken down in terms of functionality. We represent the organic nitrate group functionality as f_{ONO_2+H} and the rest of the organic group as f_{CH_2}. The presence of oxygenated groups are treated later in the main text by further breaking down the f_{CH_2} component. For the time being, this effectively represent the organic molecules as a nominal formula of $H(CH_2)_n(ONO_2)_m$. The explicit inclusion of one extra hydrogen to the $-ONO_2$ group is for valence balance of a fully saturated molecule. The resulting representation for $\widetilde{v}$ is therefore:

$$\widetilde{v} = \widetilde{v}_{dust} \times f_{dust} + \widetilde{v}_{ONO_2} \times f_{ONO_2+H} + \widetilde{v}_{CH_2} \times f_{CH_2} \qquad (A3)$$

Since it was observed that the nitrate group is a rather consistent component of the organic aerosols (Fig. 3), we expect f_{CH_2} to vary with f_{ONO_2+H} by a constant coefficient γ so that $f_{CH_2} = \gamma \times f_{ONO_2+H}$. This gives us Eq. (A4):

$$\widetilde{v} = \widetilde{v}_{dust} \times f_{dust} + \left(\widetilde{v}_{ONO_2} + \gamma \times \widetilde{v}_{CH_2}\right) \times f_{ONO_2+H} \qquad (A4)$$

By further assuming that the specific volume of the nitrate group is the same as the CH_2 fragment in a large organic molecule (subsequently called $\widetilde{v}_{org}$) and using the constraint from Eq. (A2) to substitute for f_{dust}, we arrive at Eq. (A5) which we may simplify into Eq. (A6) (or Eq. (1) in the main text) by rearrangement of terms and replacing f_{ONO_2+H} with f_{ONO_2}, since the mass of a hydrogen is small compared to the mass of a nitrooxy group.

$$\widetilde{v} = \widetilde{v}_{dust} \times [1 - (1 + \gamma) \times f_{ONO_2+H}] + (1 + \gamma) \times \widetilde{v}_{org} \times f_{ONO_2+H} \qquad (A5)$$

$$\widetilde{v} = \widetilde{v}_{dust} + \left(\widetilde{v}_{org} - \widetilde{v}_{dust}\right) \times (1 + \gamma) \times f_{ONO_2} \qquad (A6)$$

We see that Eq. (A6) predicts a linear relationship between $PM_{2.5}$ specific volume and mass fraction of the nitrooxy group in the aerosol phase, under conditions where the inorganic and organic components have relatively constant specific mass. We demonstrate that this relation is indeed observed during UBWOS 2012 in Fig. 4.

Appendix B: Estimation of ΣAN contribution using extrapolated VOC reactivity

To estimate specific contributions of organic nitrates to the aerosol formation, we traced oxidation of long-chain alkanes up to the second generation RO_2 products. Consider a simple alkane R, the dominant OH reaction is abstraction of hydrogen to give the first generation RO_2 radical which upon reaction with abundant NO during UBWOS conditition leads to alkyl nitrate compound $R(ONO_2)$ and alkoxy radical RO of relative yield α and $(1 - \alpha)$. For R with carbon chain length over 6, the isomerization dominates the fate of RO by hydrogen abstraction within the same molecule through a 6-membered ring transition state (rate constant typically $> 10^4 \, s^{-1}$). The result is a hydroxy peroxy radical upon reaction with O_2 (second generation RO_2). The same NO reaction proceeds to give a second generation hydroxy nitrate $R(OH)(ONO_2)$ and a hydroxy alkoxy radical, which may promptly react $(> 10^5 \, s^{-1})$ with the hydrogen on the hydroxy group carbon to give a hydroxy carbonyl $R(=O)(OH)$ which is assumed to represent the rest of the non-nitrate functionality under our simplification. It is also assumed that the organic nitrate yield are not affected by the presence of non-neighboring OH group to give the simplified branching ratios shown in Reactions (R B1) to (R B3). We then calculate the vapor pressure of each molecule surrogate using group contribution method SIMPOL.1, of a given carbon chain length in the R group at 273 K.

$$\alpha \qquad R + OH \rightarrow R(ONO_2) \tag{R B1}$$

$$(1 - \alpha) \times \alpha \quad R + OH \rightarrow R(OH)(ONO_2) \tag{R B2}$$

$$(1 - \alpha)^2 \qquad R + OH \rightarrow R(=O)(OH) \tag{R B3}$$
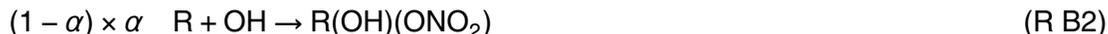
In order to obtain a converging estimation with respect to the long-carbon chain end of the VOC spectrum, it is necessary to extrapolate the contribution of heavy VOCs beyond the measurement which terminates at undecane. Using a linear fit in the log space of the grouped VOC reactivity with specific carbon number, we obtained an estimation shown in Eq. (B1) for the 30 January accumulation period where kx is the total

reactivity in unit of s^{-1} of alkanes with carbon number n.

$$\ln(kx) = -0.5893 \times n + 3.9223 \tag{B1}$$
$$S_n\{R(OH)(ONO_2)\} = kx \times [OH] \times (1 - \alpha) \times \alpha \times K_p \tag{B2}$$

The total aerosol source of each molecule type within each carbon number class is then calculated in the same way shown for the hydroxy nitrates of size n (Eq. B2). Note K_p is the fraction of the species in the aerosol phase, calculated using Eq. (2) in the main text. The total nitrate groups incorporated into the aerosol phase is the calculated by summing over all carbon groups of alkyl nitrates and hydroxy nitrates. Other functional groups is calculated similarity with application of appropriate weightings. For example, the total CH_2 group contribution is calculated according to Eq. (B3).

$$\sum_n n \times \left(S_n\{R(ONO_2)\} + S_n\{R(OH)(ONO_2)\} + S_n\{R(=O)(OH)\}\right) \tag{B3}$$

References

Arey, J., Aschmann, S. M., Kwok, E. S. C., and Atkinson, R.: Alkyl nitrate, hydroxyalkyl nitrate, and hydroxycarbonyl formation from the NO$_x$-air photooxidations of C-5-C-8 n-alkanes, J. Phys. Chem. A, 105, 1020–1027, doi:10.1021/jp003292z, 2001.

Bahreini, R., Middlebrook, A. M., de Gouw, J. A., Warneke, C., Trainer, M., Brock, C. A., Stark, H., Brown, S. S., Dube, W. P., Gilman, J. B., Hall, K., Holloway, J. S., Kuster, W. C., Perring, A. E., Prevot, A. S. H., Schwarz, J. P., Spackman, J. R., Szidat, S., Wagner, N. L., Weber, R. J., Zotter, P., and Parrish, D. D.: Gasoline emissions dominate over diesel in formation of secondary organic aerosol mass, Geophys. Res. Lett., 39, 6, doi:10.1029/2011gl050718, 2012.

Bertram, T. H., Thornton, J. A., Riedel, T. P., Middlebrook, A. M., Bahreini, R., Bates, T. S., Quinn, P. K., and Coffman, D. J.: Direct observations of N_2O_5 reactivity on ambient aerosol particles, Geophys. Res. Lett., 36, 5, doi:10.1029/2009gl040248, 2009.

Borbon, A., Gilman, J. B., Kuster, W. C., Grand, N., Chevaillier, S., Colomb, A., Dolgorouky, C., Gros, V., Lopez, M., Sarda-Esteve, R., Holloway, J., Stutz, J., Petetin, H., McKeen, S., Beekmann, M., Warneke, C., Parrish, D. D., and de Gouw, J. A.: Emission ratios of anthropogenic volatile organic compounds in northern mid-latitude megacities: observations vs. emission inventories in Los Angeles and Paris, J. Geophys. Res.-Atmos., 118, 2041–2057, doi:10.1002/jgrd.50059, 2013.

Boynard, A., Borbon, A., Leonardis, T., Barletta, B., Meinardi, S., Blake, D. R., and Locoge, N.: Spatial and seasonal variability of measured anthropogenic non-methane hydrocarbons in urban atmospheres: implication on emission ratios, Atmos. Environ., 82, 258–267, doi:10.1016/j.atmosenv.2013.09.039, 2014.

Brown, S. S., deGouw, J. A., Warneke, C., Ryerson, T. B., Dubé, W. P., Atlas, E., Weber, R. J., Peltier, R. E., Neuman, J. A., Roberts, J. M., Swanson, A., Flocke, F., McKeen, S. A., Brioude, J., Sommariva, R., Trainer, M., Fehsenfeld, F. C., and Ravishankara, A. R.: Nocturnal isoprene oxidation over the Northeast United States in summer and its impact on reactive nitrogen partitioning and secondary organic aerosol, Atmos. Chem. Phys., 9, 3027–3042, doi:10.5194/acp-9-3027-2009, 2009.

Carter, W. P. L. and Atkinson, R.: Alkyl nitrate formation from the atmospheric photooxidation of alkanes – a revised estimation method, J. Atmos. Chem., 8, 165–173, doi:10.1007/bf00053721, 1989.

Day, D. A., Wooldridge, P. J., Dillon, M. B., Thornton, J. A., and Cohen, R. C.: A thermal dissociation laser-induced fluorescence instrument for in situ detection of NO(2), peroxy nitrates, alkyl nitrates, and HNO(3), J. Geophys. Res.-Atmos., 107, ACH 4-1-ACH 4-14, doi:10.1029/2001jd000779, 2002.

Day, D. A., Liu, S., Russell, L. M., and Ziemann, P. J.: Organonitrate group concentrations in submicron particles with high nitrate and organic fractions in coastal southern California, Atmos. Environ., 44, 1970–1979, doi:10.1016/j.atmosenv.2010.02.045, 2010.

de Gouw, J. A., Middlebrook, A. M., Warneke, C., Ahmadov, R., Atlas, E. L., Bahreini, R., Blake, D. R., Brock, C. A., Brioude, J., Fahey, D. W., Fehsenfeld, F. C., Holloway, J. S., Le Henaff, M., Lueb, R. A., McKeen, S. A., Meagher, J. F., Murphy, D. M., Paris, C., Parrish, D. D., Perring, A. E., Pollack, I. B., Ravishankara, A. R., Robinson, A. L., Ry-

Particulate organic nitrates observed in an oil and natural gas production region

L. Lee et al.

Title Page

Abstract · Introduction

Conclusions · References

Tables · Figures

|◄ · ►|

◄ · ►

Back · Close

Full Screen / Esc

Printer-friendly Version

Interactive Discussion

erson, T. B., Schwarz, J. P., Spackman, J. R., Srinivasan, A., and Watts, L. A.: Organic aerosol formation downwind from the Deepwater Horizon oil spill, Science, 331, 1295–1299, doi:10.1126/science.1200320, 2011.

Edwards, P. M., Young, C. J., Aikin, K., deGouw, J., Dubé, W. P., Geiger, F., Gilman, J., Helmig, D., Holloway, J. S., Kercher, J., Lerner, B., Martin, R., McLaren, R., Parrish, D. D., Peischl, J., Roberts, J. M., Ryerson, T. B., Thornton, J., Warneke, C., Williams, E. J., and Brown, S. S.: Ozone photochemistry in an oil and natural gas extraction region during winter: simulations of a snow-free season in the Uintah Basin, Utah, Atmos. Chem. Phys., 13, 8955–8971, doi:10.5194/acp-13-8955-2013, 2013.

Farmer, D. K., Matsunaga, A., Docherty, K. S., Surratt, J. D., Seinfeld, J. H., Ziemann, P. J., and Jimenez, J. L.: Response of an aerosol mass spectrometer to organonitrates and organosulfates and implications for atmospheric chemistry, P. Natl. Acad. Sci. USA, 107, 6670–6675, doi:10.1073/pnas.0912340107, 2010.

Froyd, K. D., Murphy, S. M., Murphy, D. M., de Gouw, J. A., Eddingsaas, N. C., and Wennberg, P. O.: Contribution of isoprene-derived organosulfates to free tropospheric aerosol mass, P. Natl. Acad. Sci. USA, 107, 21360–21365, doi:10.1073/pnas.1012561107, 2010.

Garnes, L. A. and Allen, D. T.: Size distributions of organonitrates in ambient aerosol collected in Houston, Texas, Aerosol Sci. Technol., 36, 983–992, doi:10.1080/02786820290092186, 2002.

Gentner, D. R., Isaacman, G., Worton, D. R., Chan, A. W. H., Dallmann, T. R., Davis, L., Liu, S., Day, D. A., Russell, L. M., Wilson, K. R., Weber, R., Guha, A., Harley, R. A., and Goldstein, A. H.: Elucidating secondary organic aerosol from diesel and gasoline vehicles through detailed characterization of organic carbon emissions, P. Natl. Acad. Sci. USA, 109, 18318–18323, doi:10.1073/pnas.1212272109, 2012.

Goldstein, A. H. and Galbally, I. E.: Known and unexplored organic constituents in the Earth's atmosphere, Environ. Sci. Technol., 41, 1514–1521, doi:10.1021/es072476p, 2007.

Gordon, T. D., Tkacik, D. S., Presto, A. A., Zhang, M., Jathar, S. H., Nguyen, N. T., Massetti, J., Tin, T., Cicero-Fernandez, P., Maddox, C., Rieger, P., Chattopadhyay, S., Maldonado, H., Maricq, M. M., and Robinson, A. L.: Primary gas- and particle-phase emissions and secondary organic aerosol production from gasoline and diesel off-road engines, Environ. Sci. Technol., 47, 14137–14146, doi:10.1021/es403556e, 2013.

Particulate organic nitrates observed in an oil and natural gas production region

L. Lee et al.

Title Page

Abstract	Introduction
Conclusions	References
Tables	Figures

◀◀ | ▶▶

◀ | ▶

Back | Close

Full Screen / Esc

Printer-friendly Version

Interactive Discussion

Gross, S., Iannone, R., Xiao, S., and Bertram, A. K.: Reactive uptake studies of NO(3) and N(2)O(5) on alkenoic acid, alkanoate, and polyalcohol substrates to probe nighttime aerosol chemistry, Phys. Chem. Chem. Phys., 11, 7792–7803, doi:10.1039/b904741g, 2009.

Hallquist, M., Wenger, J. C., Baltensperger, U., Rudich, Y., Simpson, D., Claeys, M., Dommen, J., Donahue, N. M., George, C., Goldstein, A. H., Hamilton, J. F., Herrmann, H., Hoffmann, T., Iinuma, Y., Jang, M., Jenkin, M. E., Jimenez, J. L., Kiendler-Scharr, A., Maenhaut, W., McFiggans, G., Mentel, Th. F., Monod, A., Prévôt, A. S. H., Seinfeld, J. H., Surratt, J. D., Szmigielski, R., and Wildt, J.: The formation, properties and impact of secondary organic aerosol: current and emerging issues, Atmos. Chem. Phys., 9, 5155–5236, doi:10.5194/acp-9-5155-2009, 2009.

Jathar, S. H., Miracolo, M. A., Tkacik, D. S., Donahue, N. M., Adams, P. J., and Robinson, A. L.: Secondary organic aerosol formation from photo-oxidation of unburned fuel: experimental results and implications for aerosol formation from combustion emissions, Environ. Sci. Technol., 47, 12886–12893, doi:10.1021/es403445q, 2013.

Jordan, C. E., Ziemann, P. J., Griffin, R. J., Lim, Y. B., Atkinson, R., and Arey, J.: Modeling SOA formation from OH reactions with C-8-C-17 n-alkanes, Atmos. Environ., 42, 8015–8026, doi:10.1016/j.atmosenv.2008.06.017, 2008.

Kleinman, M. T., Bhalla, D. K., Mautz, W. J., and Phalen, R. F.: Cellular and immunological injury with PM_{10} inhalation, Inhal. Toxicol., 7, 589–602, doi:10.3109/08958379509014467, 1995.

Kwok, E. S. C. and Atkinson, R.: Estimation of hydroxyl radical reaction-rate constants for gas-phase organic-compounds using a structure–reactivity relationship – an update, Atmos. Environ., 29, 1685–1695, doi:10.1016/1352-2310(95)00069-b, 1995.

Lee, L., Wooldridge, P., Nah, T., Wilson, K., and Cohen, R.: Observation of rates and products in the reaction of NO_3 with submicron squalane and squalene aerosol, Phys. Chem. Chem. Phys., 15, 882–892, doi:10.1039/c2cp42500a, 2013.

Lee, L., Wooldridge, P. J., Gilman, J. B., Warneke, C., de Gouw, J., and Cohen, R. C.: Low temperatures enhance organic nitrate formation: evidence from observations in the 2012 Uintah Basin Winter Ozone Study, Atmos. Chem. Phys., 14, 12441–12454, doi:10.5194/acp-14-12441-2014, 2014.

Lewis, C. W., Klouda, G. A., and Ellenson, W. D.: Radiocarbon measurement of the biogenic contribution to summertime PM-2.5 ambient aerosol in Nashville, TN, Atmos. Environ., 38, 6053–6061, doi:10.1016/j.atmosenv.2004.06.011, 2004.

Title Page

Abstract | Introduction

Conclusions | References

Tables | Figures

◀ | ▶|

◀ | ▶

Back | Close

Full Screen / Esc

Printer-friendly Version

Interactive Discussion

Lim, Y. B. and Ziemann, P. J.: Chemistry of secondary organic aerosol formation from OH radical-initiated reactions of linear, branched, and cyclic alkanes in the presence of NO_x, Aerosol Sci. Technol., 43, 604–619, doi:10.1080/02786820902802567, 2009.

Matsunaga, A. and Ziemann, P. J.: Yields of beta-hydroxynitrates, dihydroxynitrates, and trihy-droxynitrates formed from OH radical-initiated reactions of 2-methyl-1-alkenes, P. Natl. Acad. Sci. USA, 107, 6664–6669, doi:10.1073/pnas.0910585107, 2010.

Mylonas, D. T., Allen, D. T., Ehrman, S. H., and Pratsinis, S. E.: The sources and size dis-tributions of organonitrates in Los-Angeles aerosol, Atmos. Environ. A, 25, 2855–2861, doi:10.1016/0960-1686(91)90211-o, 1991.

Pankow, J. F. and Asher, W. E.: SIMPOL.1: a simple group contribution method for predicting vapor pressures and enthalpies of vaporization of multifunctional organic compounds, Atmos. Chem. Phys., 8, 2773–2796, doi:10.5194/acp-8-2773-2008, 2008.

Paulot, F., Crounse, J. D., Kjaergaard, H. G., Kuerten, A., St Clair, J. M., Seinfeld, J. H., and Wennberg, P. O.: Unexpected epoxide formation in the gas-phase photooxidation of isoprene, Science, 325, 730–733, doi:10.1126/science.1172910, 2009.

Roberts, J. M., Osthoff, H. D., Brown, S. S., Ravishankara, A. R., Coffman, D., Quinn, P., and Bates, T.: Laboratory studies of products of N_2O_5 uptake on Cl^- containing substrates, Geo-phys. Res. Lett., 36, L20808, doi:10.1029/2009gl040448, 2009.

Rollins, A. W., Kiendler-Scharr, A., Fry, J. L., Brauers, T., Brown, S. S., Dorn, H.-P., Dubé, W. P., Fuchs, H., Mensah, A., Mentel, T. F., Rohrer, F., Tillmann, R., Wegener, R., Wooldridge, P. J., and Cohen, R. C.: Isoprene oxidation by nitrate radical: alkyl nitrate and secondary organic aerosol yields, Atmos. Chem. Phys., 9, 6685–6703, doi:10.5194/acp-9-6685-2009, 2009.

Rollins, A. W., Fry, J. L., Hunter, J. F., Kroll, J. H., Worsnop, D. R., Singaram, S. W., and Cohen, R. C.: Elemental analysis of aerosol organic nitrates with electron ionization high-resolution mass spectrometry, Atmos. Meas. Tech., 3, 301–310, doi:10.5194/amt-3-301-2010, 2010a.

Rollins, A. W., Smith, J. D., Wilson, K. R., and Cohen, R. C.: Real time in situ detec-tion of organic nitrates in atmospheric aerosols, Environ. Sci. Technol., 44, 5540–5545, doi:10.1021/es100926x, 2010b.

Rollins, A. W., Browne, E. C., Min, K. E., Pusede, S. E., Wooldridge, P. J., Gentner, D. R., Goldstein, A. H., Liu, S., Day, D. A., Russell, L. M., and Cohen, R. C.: Evidence for NO_x con-trol over nighttime SOA formation, Science, 337, 1210–1212, doi:10.1126/science.1221520, 2012.

Particulate organic nitrates observed in an oil and natural gas production region

L. Lee et al.

Title Page

Abstract | Introduction

Conclusions | References

Tables | Figures

|◄ | ►|

◄ | ►

Back | Close

Full Screen / Esc

Printer-friendly Version

Interactive Discussion

Rollins, A. W., Pusede, S., Wooldridge, P., Min, K. E., Gentner, D. R., Goldstein, A. H., Liu, S., Day, D. A., Russell, L. M., Rubitschun, C. L., Surratt, J. D., and Cohen, R. C.: Gas/particle partitioning of total alkyl nitrates observed with TD-LIF in Bakersfield, J. Geophys. Res.-Atmos., 118, 6651–6662, doi:10.1002/jgrd.50522, 2013.

5   Shilling, J. E., Zaveri, R. A., Fast, J. D., Kleinman, L., Alexander, M. L., Canagaratna, M. R., Fortner, E., Hubbe, J. M., Jayne, J. T., Sedlacek, A., Setyan, A., Springston, S., Worsnop, D. R., and Zhang, Q.: Enhanced SOA formation from mixed anthropogenic and biogenic emissions during the CARES campaign, Atmos. Chem. Phys., 13, 2091–2113, doi:10.5194/acp-13-2091-2013, 2013.

10   Steiner, A. L., Cohen, R. C., Harley, R. A., Tonse, S., Millet, D. B., Schade, G. W., and Goldstein, A. H.: VOC reactivity in central California: comparing an air quality model to ground-based measurements, Atmos. Chem. Phys., 8, 351–368, doi:10.5194/acp-8-351-2008, 2008.

Szidat, S., Jenk, T. M., Gaggeler, H. W., Synal, H. A., Fisseha, R., Baltensperger, U., Kalberer, M., Samburova, V., Reimann, S., Kasper-Giebl, A., and Hajdas, I.: Radiocarbon (C^{14})-deduced biogenic and anthropogenic contributions to organic carbon (OC) of urban aerosols from Zurich, Switzerland, Atmos. Environ., 38, 4035–4044, doi:10.1016/j.atmosenv.2004.03.066, 2004.

Thornton, J. A., Wooldridge, P. J., and Cohen, R. C.: Atmospheric NO_2: in situ laser-induced fluorescence detection at parts per trillion mixing ratios, Anal. Chem., 72, 528–539, doi:10.1021/ac9908905, 2000.

Wagner, N. L., Dubé, W. P., Washenfelder, R. A., Young, C. J., Pollack, I. B., Ryerson, T. B., and Brown, S. S.: Diode laser-based cavity ring-down instrument for NO_3, N_2O_5, NO, NO_2 and O_3 from aircraft, Atmos. Meas. Tech., 4, 1227–1240, doi:10.5194/amt-4-1227-2011, 2011.

25   Weber, R. J., Sullivan, A. P., Peltier, R. E., Russell, A., Yan, B., Zheng, M., de Gouw, J., Warneke, C., Brock, C., Holloway, J. S., Atlas, E. L., and Edgerton, E.: A study of secondary organic aerosol formation in the anthropogenic-influenced southeastern United States, J. Geophys. Res.-Atmos., 112, 13, doi:10.1029/2007jd008408, 2007.

Went, F. W.: Blue hazes in the atmosphere, Nature, 187, 641–643, doi:10.1038/187641a0, 1960.

Williams, J., Roberts, J. M., Bertman, S. B., Stroud, C. A., Fehsenfeld, F. C., Baumann, K., Buhr, M. P., Knapp, K., Murphy, P. C., Nowick, M., and Williams, E. J.: A method for the

Particulate organic nitrates observed in an oil and natural gas production region

L. Lee et al.

Title Page

Abstract | Introduction

Conclusions | References

Tables | Figures

|◄ | ►|

◄ | ►

Back | Close

Full Screen / Esc

Printer-friendly Version

Interactive Discussion

airborne measurement of PAN, PPN, and MPAN, J. Geophys. Res.-Atmos., 105, 28943–28960, doi:10.1029/2000jd900373, 2000.

Worton, D. R., Surratt, J. D., LaFranchi, B. W., Chan, A. W. H., Zhao, Y. L., Weber, R. J., Park, J. H., Gilman, J. B., de Gouw, J., Park, C., Schade, G., Beaver, M., St Clair, J. M., Crounse, J., Wennberg, P., Wolfe, G. M., Harrold, S., Thornton, J. A., Farmer, D. K., Docherty, K. S., Cubison, M. J., Jimenez, J. L., Frossard, A. A., Russell, L. M., Kristensen, K., Glasius, M., Mao, J. Q., Ren, X. R., Brune, W., Browne, E. C., Pusede, S. E., Cohen, R. C., Seinfeld, J. H., and Goldsteint, A. H.: Observational insights into aerosol formation from isoprene, Environ. Sci. Technol., 47, 11403–11413, doi:10.1021/es4011064, 2013.

Worton, D. R., Isaacman, G., Gentner, D. R., Dallmann, T. R., Chan, A. W. H., Ruehl, C., Kirchstetter, T. W., Wilson, K. R., Harley, R. A., and Goldstein, A. H.: Lubricating oil dominates primary organic aerosol emissions from motor vehicles, Environ. Sci. Technol., 48, 3698–3706, doi:10.1021/es405375j, 2014.

Xiao, S. and Bertram, A. K.: Reactive uptake kinetics of NO(3) on multicomponent and multiphase organic mixtures containing unsaturated and saturated organics, Phys. Chem. Chem. Phys., 13, 6628–6636, doi:10.1039/c0cp02682d, 2011.

Zhang, Q., Jimenez, J. L., Canagaratna, M. R., Allan, J. D., Coe, H., Ulbrich, I., Alfarra, M. R., Takami, A., Middlebrook, A. M., Sun, Y. L., Dzepina, K., Dunlea, E., Docherty, K., De-Carlo, P. F., Salcedo, D., Onasch, T., Jayne, J. T., Miyoshi, T., Shimono, A., Hatakeyama, S., Takegawa, N., Kondo, Y., Schneider, J., Drewnick, F., Borrmann, S., Weimer, S., Demerjian, K., Williams, P., Bower, K., Bahreini, R., Cottrell, L., Griffin, R. J., Rautiainen, J., Sun, J. Y., Zhang, Y. M., and Worsnop, D. R.: Ubiquity and dominance of oxygenated species in organic aerosols in anthropogenically-influenced Northern Hemisphere midlatitudes, Geophys. Res. Lett., 34, 6, doi:10.1029/2007gl029979, 2007.

Zhang, Y. L., Zotter, P., Perron, N., Prevot, A. S. H., Wacker, L., and Szidat, S.: Fossil and non-fossil sources of different carbonaceous fractions in fine and coarse particles by radiocarbon measurement, Radiocarbon, 55, 1510–1520, doi:10.2458/azu_js_rc.55.16278, 2013.

Zhao, Z. J., Husainy, S., and Smith, G. D.: Kinetics studies of the gas-phase reactions of NO_3 radicals with series of 1-alkenes, dienes, cycloalkenes, alkenols, and alkenals, J. Phys. Chem. A, 115, 12161–12172, doi:10.1021/jp206899w, 2011a.

Zhao, Z. J., Husainy, S., Stoudemayer, C. T., and Smith, G. D.: Reactive uptake of NO(3) radicals by unsaturated fatty acid particles, Phys. Chem. Chem. Phys., 13, 17809–17817, doi:10.1039/c1cp21790a, 2011b.

Title Page

Abstract | Introduction

Conclusions | References

Tables | Figures

|◄ | ►|

◄ | ►

Back | Close

Full Screen / Esc

Printer-friendly Version

Interactive Discussion
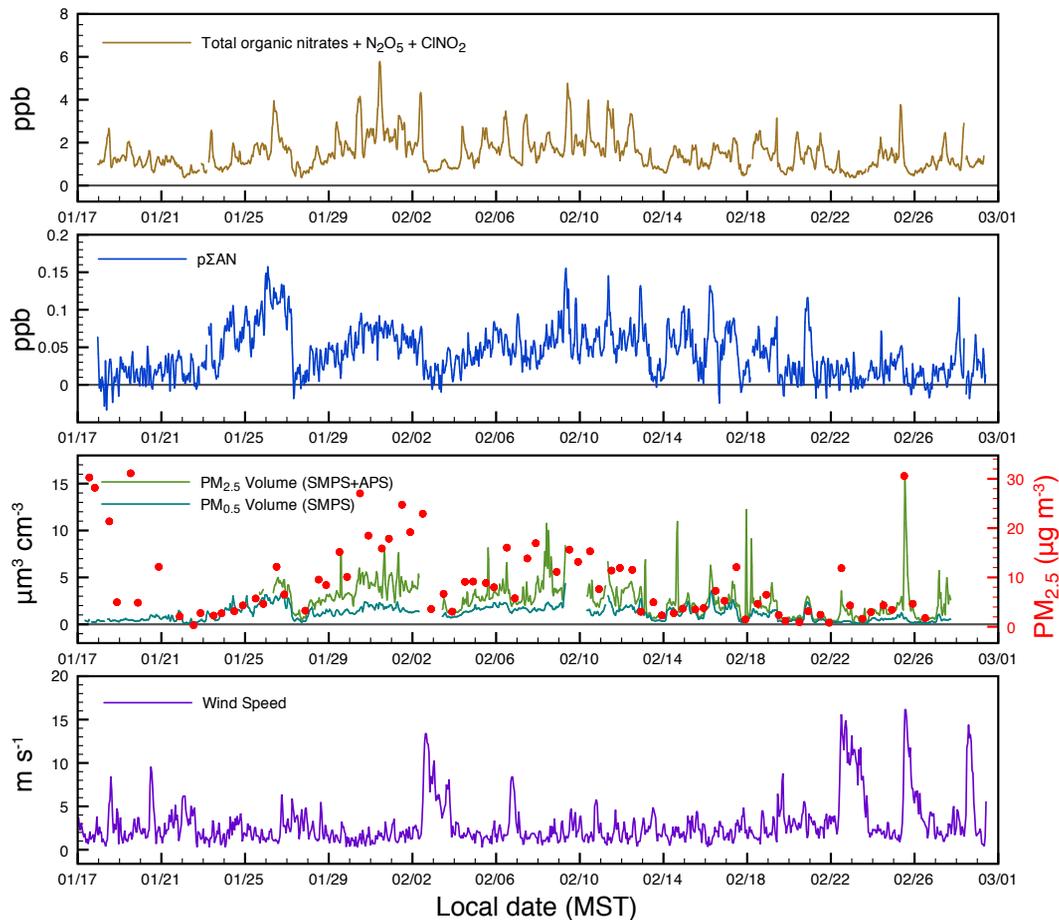
Figure 1. Hourly time series from measurements of total organic nitrates plus N_2O_5 and $ClNO_2$, particulate organic nitrate (pΣAN), total aerosol volume measured by SMPS and APS with filter sampled $PM_{2.5}$ mass (red dot, secondary axis) and local wind speed.
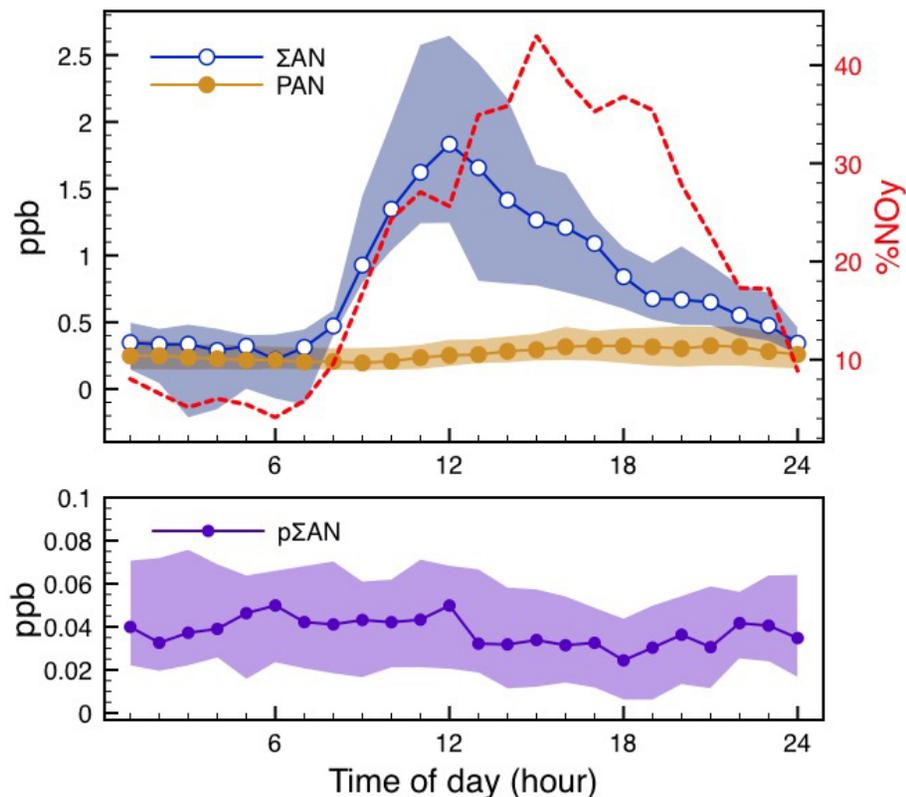
Figure 2. Average mixing ratios of total alkyl nitrate (ΣAN, blue), PAN (yellow), (ΣAN/NO_y) × 100 % (red dashed) and pΣAN (purple) v.s. time of day. Inter-quartile range is shaded.

Particulate organic nitrates observed in an oil and natural gas production region
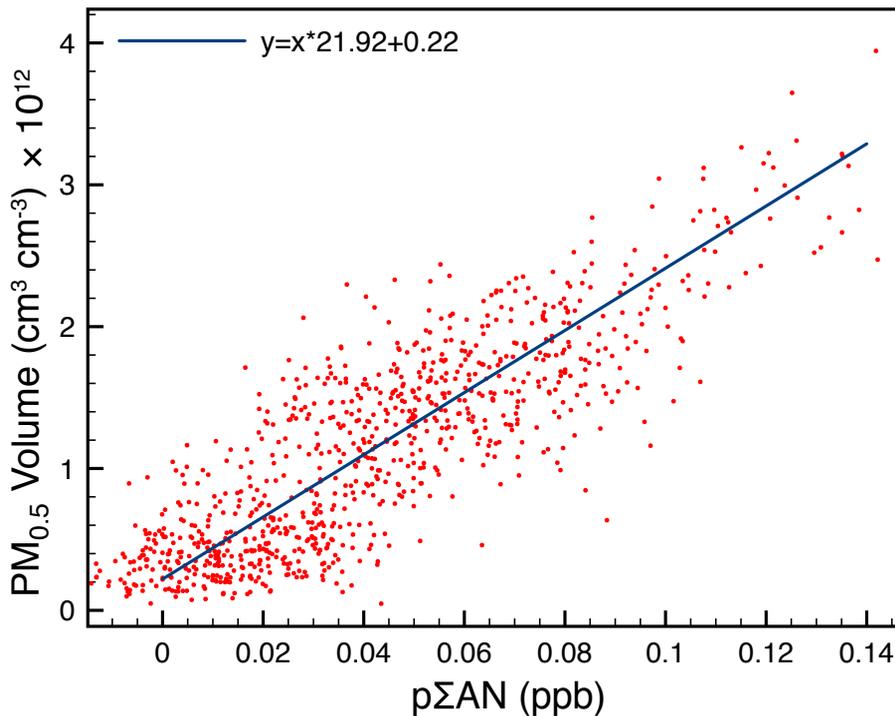
L. Lee et al.

Figure 3. Correlation of $PM_{0.5}$ volume measured by SMPS to particulate organic nitrate concentration ($R^2 = 0.72$).
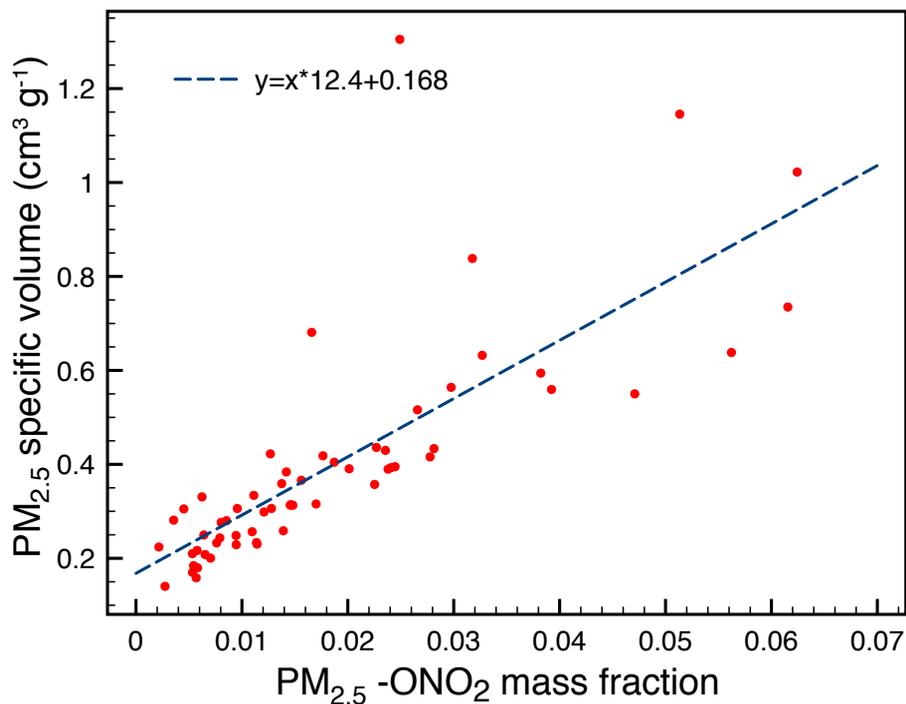
Figure 4. Correlation of specific volume (inverse density) to the mass fraction of the aerosol organic nitrate for $PM_{2.5}$ size range ($R^2 = 0.6$).
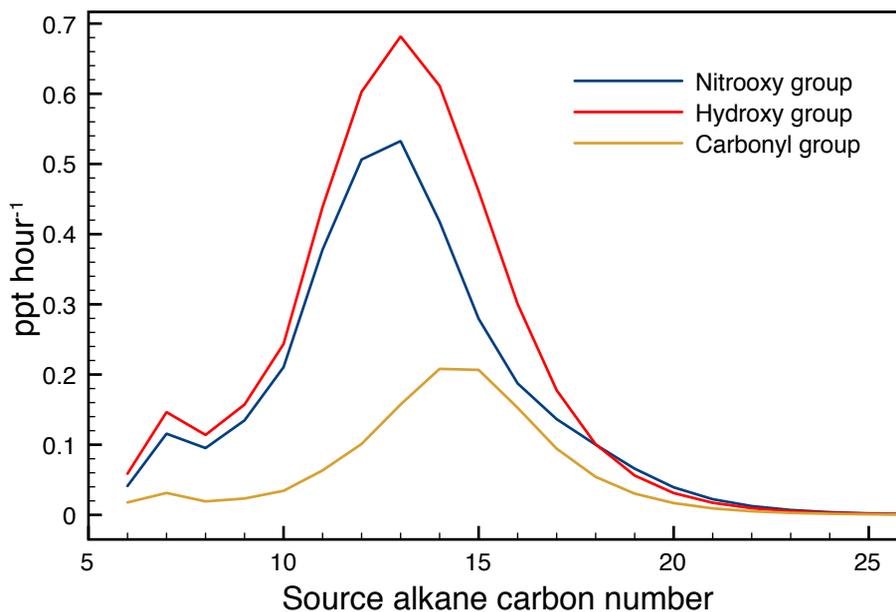
Figure 5. Source strength of functional groups for molecules contributing to aerosol formation on 30 January categorized by carbon number.
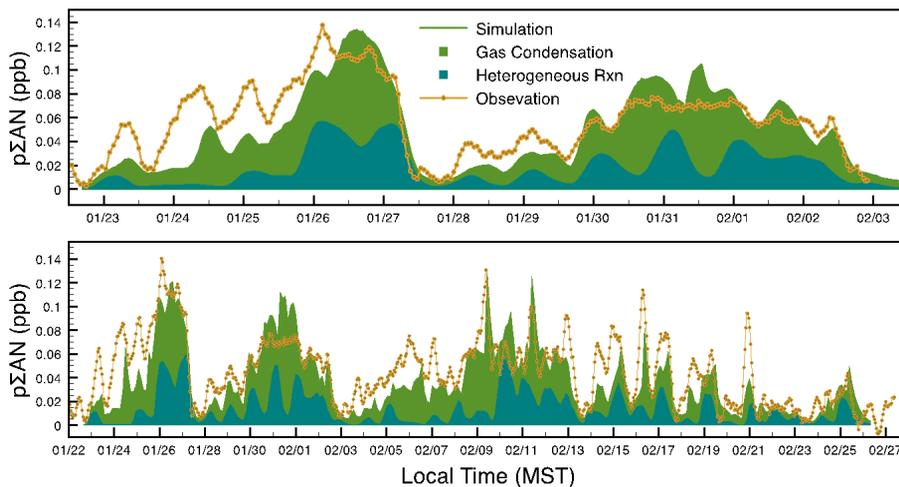
Figure 6. Time series of predicted particulate organic nitrate concentration from box model simulation for 2 accumulation events (top panel) and the campaign period (bottom panel) as stacked areas showing contribution from each of the 2 mechanisms responsible. The observations are plotted in yellow.